J|A|C|S
ARTICLES

Published on Web 11/06/2009

Iron-Porphyrin NO Complexes with Covalently Attached N-Donor Ligands: Formation of a Stable Six-Coordinate Species in Solution

Timothy C. Berto, V. K. K. Praneeth, Lauren E. Goodrich, and Nicolai Lehnert*

Department of Chemistry, University of Michigan, Ann Arbor, Michigan 48109

Received May 29, 2009; E-mail: lehnertn@umich.edu

Abstract: A series of substituted tetraphenylporphyrin type macrocycles (TMP or T*o*-F_2PP) with covalently attached N-donor ligands (pyridine or imidazole linker) have been synthesized. Linkers with varying chain lengths and designs have been applied to systematically investigate the effect of chain length and rigidity on the binding affinity of the linker to the corresponding Fe(II)−NO heme complexes. The binding of the linker is monitored in solution using a variety of spectroscopic methods including UV−vis absorption, EPR, and IR spectroscopy. Both the N−O stretching frequency and the imidazole ^{14}N hyperfine coupling constants show a good correlation with the Fe−(N-donor) bond strength in these systems. The complexes with covalently attached pyridyl and alkyl imidazole ligands only exhibit weak interactions of the linker with iron(II). However, the stable six-coordinate complex [Fe(T*o*-F_2PP-BzIM)(NO)] (**4**) is obtained when a rigid benzyl linker is applied. This complex exhibits typical properties of six-coordinate ferrous heme-nitrosyls in which an N-donor ligand is bound *trans* to NO, including the Soret band at 427 nm and the typical nine line ^{14}N hyperfine splitting in the EPR spectrum. A crystal structure has been obtained for the corresponding zinc complex. Here, we report the first systematic study on the requirements for the formation of stable six-coordinate ferrous heme nitrosyl complexes in solution at room temperature in the absence of excess axial N-donor ligand.

Introduction

Heme proteins are involved in many important biological processes, including electron transfer, catalysis, and signaling. Many of these functions involve the interaction of ferrous hemes with diatomics, in particular O_2, NO, and CO.[1] Because of the exceptional significance of heme diatomic interactions, much research has been devoted to the synthesis of model complexes for the corresponding heme proteins. In many cases, a proximal histidine is present as the trans ligand to the diatomic bound at the distal site. Prominent examples of this structural motif are found in the O_2 transport and storage proteins hemoglobin (Hb) and myoglobin (Mb), the NO sensor soluble guanylate cyclase (sGC), and peroxidases.[2] A similar active site with a copper center in close proximity is also found in cytochrome c oxidase (CcO). Here, the heme-copper center binds and reduces dioxygen, and thus facilitates respiration within living organisms. Finally, the active site of bacterial nitric oxide reductase (NorBC) contains a heme with axial histidine coordination, which has been proposed to influence the binding and reactivity of NO bound at the distal site.[3] Because of this, many synthetic model complexes, for example those of Mb, Hb, CcO, and NorBC, have been equipped with pyridine (Py) or imidazole (IM) type ligands that are covalently tethered to the porphyrin core in order to model this proximal histidine.[4]

Model systems of biological hemes that include the proximal histidine usually consist of a modified synthetic porphyrin with a covalently tethered N-donor ligand.[4] Original work in this field, carried out by Traylor and co-workers, led to the development of the so-called "cyclophane" porphyrins[5] in which alkyl imidazole or thiolate linked chains were anchored at the β-pyrrole positions of protoheme.[6,4d,7] These models served as mimics for the active sites of globins and peroxidases. In separate studies, tethers at the β-pyrrole positions of porphyrin ligands have also been used to covalently connect two separate hemes via peptide linkages.[8] Work by Dolphin and co-workers focused on the investigation of the electronic structure of such dimeric porphyrin species as a function of the length of the

(1) *The Smallest Biomolecules: Diatomics and their Interactions with Heme Proteins*; Ghosh, A., Ed.; Elsevier: Amsterdam, 2008.
(2) (a) Garbers, D. L.; Lowe, D. G. *J. Biol. Chem.* **1996**, *269*, 30741–30744. (b) Waldman, S. A.; Murad, F. *Pharmacol. Rev.* **1987**, *39*, 163–196. (c) Riggs, A. F. *Curr. Opin. Struct. Biol.* **1991**, *1*, 915. (d) Hersleth; et al. *Inorg. Chim. Acta* **2008**, *361*, 831–843.
(3) Moënne-Loccoz, P.; de Vries, S. *J. Am. Chem. Soc.* **1998**, *120*, 5147–5152.
(4) See refs in: (a) Walker, F. A.; Simonis, U. Iron Porphyrin Chemistry. In: *Encyclopedia of Inorganic Chemistry*, 2nd ed.; King, R. B., Ed.; John Wiley & Sons, Ltd.: Chichester, 2005; Vol. IV, p 2390. (b) Collman, J. P.; Boulatov, R. ; Sunderland, C. J.; Fu, L. *Chem. Rev.* **2004**, *104*, 561. (c) Kim, E.; Chufán, E. E.; Kamaraj, K.; Karlin, K. D. *Chem. Rev.* **2004**, *104*, 1077. (d) Traylor, T. G. *Acc. Chem. Res.* **1981**, *14*, 102.
(5) Traylor, T. G.; Diekmann, H.; Chang, C. K. *J. Am. Chem. Soc.* **1971**, *93*, 4068–4070.
(6) (a) Traylor, T. G.; Chang, C. K.; Geibel, J.; Berzinis, A.; Mincey, T.; Cannon, J. *J. Am. Chem. Soc.* **1979**, *101*, 6716–6731. (b) Chang, C. K.; Traylor, T. G. *Proc. Natl. Acad. Sci. U.S.A.* **1973**, *70*, 2847–2650. (c) Chang, C. K.; Traylor, T. G. *J. Am. Chem. Soc.* **1973**, *95*, 5810–5811.
(7) Traylor, T. G. *Pure Appl. Chem.* **1991**, *63*, 265–274.
(8) Schwarz, F. P.; Gouternam, M.; Muljiani, Z.; Dolphin, D. H. *Bioinorg. Chem.* **1972**, *2*, 1–32.

10.1021/ja904368n CCC: $40.75

$(CH_2)_n$ tether ($n = 0-8$).[9] Later, Momenteau and co-workers were able to improve the solubility of imidazole-tethered protohemes through the use of propionic acid side chains.[6b,10] While a considerable amount of insight has been gained from these β-pyrrole and propionic acid tethered model systems, they have been shown to exhibit undesirable intermolecular binding through the tethered donor ligands.[10] As an alternative, the use of tetraphenylporphyrin derivatives offers a convenient strategy for attaching such tethers by substituting the *ortho* positions of the *meso*-phenyl groups available in these systems. These models offer the distinct benefit that, due to the perpendicular orientation of the phenyl rings with respect to the porphyrin plane, *ortho*-phenyl substituents are conveniently directed toward the axial positions of the heme center and thus, intermolecular interactions are avoided. Collman and co-workers have shown the utility of such systems through their use of multitethered "picket fence porphyrins" which employ either ether or amide linkages.[11−13] Walker and co-workers have also utilized such porphyrin model systems to elucidate the properties of cytochromes *c*, *b*, and a_3 with respect to axial N-donor ligand geometry.[14,4a,15] Recently, model systems from the Collman, Karlin, and Naruta groups have continued to exploit the effectiveness of *meso*-phenyl tethered porphyrin systems in their models for the active site of cytochrome c oxidase.[16−19]

Our particular interest is focused on bacterial nitric oxide reductase (NorBC) which is an enzyme found in soil dwelling bacteria that is responsible for the conversion of nitric oxide (NO) to nitrous oxide (N_2O) via a two-electron reduction:

$$2NO + 2e^- + 2H^+ \rightarrow N_2O + H_2O \qquad (1)$$

This enzyme fulfills a vital role in the process of denitrification where nitrate is reduced in a stepwise fashion to dinitrogen.[20] The site of catalytic NO reduction within the enzyme consists of a dinuclear iron center with both heme and nonheme type coordination. The nonheme iron site has three histidine ligands and has been proposed to also contain glutamate ligation.[21] Located 3.5 Å from the nonheme iron is a heme *b* site with additional proximal histidine ligation similar to that seen in the heme active sites of Hb and Mb. The dimetallic heme/nonheme motif is catalytically active in the diferrous form.[20] Detailed investigations into the properties and reactivity of the heme component of the active site of NorBC could, in principle, be based on the Mb and Hb model complexes described above. However, in the case of NorBC, the interaction of NO, rather than O_2 or CO, with ferrous heme model complexes needs to be studied to arrive at a detailed structural and mechanistic understanding of this enzyme. This has important consequences for the design of model systems as the generation of six-coordinate (6C) ferrous heme nitrosyls constitutes a significant challenge.

The question of axial ligand binding is of direct relevance for the reactivity of ferrous heme nitrosyls. It has been shown that the trans ligand modulates the amount of radical character on the NO, and hence, the chemical behavior of these complexes. This is evident from spectroscopic studies including EPR, MCD, vibrational spectroscopy (coupled to normal coordinate analysis), and DFT calculations on five- and six-coordinate ferrous heme nitrosyl model systems.[22] In five-coordinate (5C) complexes a strong Fe−NO σ-bond is present between the singly occupied π^* orbital of NO and d_{z^2} of Fe(II).[22a,b] Additional backbonding is observed between the d_{xz} and d_{yz} orbitals of iron and the remaining unoccupied π^* orbital of NO. The strong σ-bond and substantial sharing of the unpaired electron via the d_{z^2} orbital of iron gives rise to the strong *σ-trans* interaction between NO and the proximal N-donor ligand in the corresponding 6C complexes. This has two consequences: (a) the binding of axial ligands trans to NO is weak, and (b) upon coordination of an N-donor ligand trans to NO, the Fe−NO bond is weakened and the unpaired electron is pushed back from the iron(II) to the NO ligand resulting in an electronic structure with Fe(II)−NO(radical) character in the 6C case.[22a,b] In this way, the N-donor ligand could help to activate the bound NO for catalysis. This is particularly relevant for the activation of NO in NorBC since ferrous heme nitrosyls are intrinsically stable and unreactive.[23]

To investigate this point further, 6C ferrous heme nitrosyl model complexes that are stable *in solution at room temperature* are needed. This is challenging because the binding constants of N-donor ligands trans to NO are generally very small ($K_{eq} \approx 1$ to 30 M^{-1}) due to the *σ-trans* effect detailed above.[22b,24] This is very different compared to CO and O_2 complexes where such a *trans* effect is lacking. Correspondingly, a recent report on Fe(II)−NO complexes of protoheme with covalently linked IM shows that these complexes are indeed only 5C in solution.[25] In fact, only one model complex is known so far where the covalently tethered N-donor ligand seems to remain bound to iron(II) after coordination of NO without the formation of 5C species in solution.[26] Systematic investigations to optimize axial ligand binding properties in tailed ferrous heme nitrosyl model systems are completely lacking. It is apparent from the literature

(9) Paine, J. B., III; Dolphin, D. *Can. J. Chem.* **1978**, *56*, 1710–1712.
(10) Momenteau, M.; Rougee, M.; Loock, B. *Eur. J. Biochem.* **1976**, *71*, 63–76.
(11) Collman, J. P.; Gagne, R. R.; Halbert, T. R.; Marchon, J. C.; Redd, C. A. *J. Am. Chem. Soc.* **1973**, *95*, 7868–7870.
(12) Collman, J. P.; Gagne, R. R.; Reed, C. A. *J. Am. Chem. Soc.* **1974**, *96*, 2629–2631.
(13) Gerothanassis, I. P.; Momenteau, M.; Barrie, P. J.; Kalodimos, C. G.; Hawkes, G. E. *Inorg. Chem.* **1996**, *35*, 2674–2679.
(14) Safo, M. K.; Gupta, G. P.; Walker, F. A.; Scheidt, W. R. *J. Am. Chem. Soc.* **1991**, *113*, 5497.
(15) Walker, F. A.; Reis, D.; Balke, V. L. *J. Am. Chem. Soc.* **1984**, *106*, 6888–6898.
(16) Kopf, M. A.; Karlin, K. D. *Inorg. Chem.* **1999**, *38*, 4922–4923.
(17) Kim, E.; Shearer, J.; Lu, S.; Moënne-Loccoz, P.; Helton, M. E.; Kaderli, S.; Zuberbhler, A. D.; Karlin, K. D. *J. Am. Chem. Soc.* **2004**, *126*, 12716–12717.
(18) Liu, J.-G.; Naruta, Y.; Tani, F. *Angew. Chem.* **2005**, *117*, 1870–1874.
(19) (a) Collman, J. P.; Ghosh, S.; Dey, A.; Decreau, R. A.; Yang, Y. *J. Am. Chem. Soc.* **2009**, *131*, 5034–5035. (b) Collman, J. P.; Fu, L.; Herrmann, P. C.; Zhang, X. *Science* **1997**, *275*, 949–951. (c) Collman, J. P.; Devaraj, N. K.; Decreau, R. A.; Yang, Y.; Yan, Y.-L.; Ebina, W.; Eberspacher, T. A.; Chidsey, C. E. D. *Science* **2007**, *315*, 1565–1568. (d) Collman, J. P.; Dey, A.; Decreau, R. A.; Yang, Y.; Hosseini, A.; Solomon, E. I.; Eberspacher, T. A. *Proc. Natl. Acad. Sci. U.S.A.* **2008**, *105*, 9892–9896.
(20) Zumft, W. G. *J. Inorg. Biochem.* **2005**, *99*, 194–215.
(21) Butland, G.; Spiro, S.; Watmough, N. J.; Richardson, D. J. *J. Bacteriol.* **2001**, *183*, 189–199.
(22) (a) Praneeth, V. K. K.; Neese, F.; Lehnert, N. *Inorg. Chem.* **2005**, *44*, 2570. (b) Praneeth, V. K. K.; Näther, C.; Peters, G.; Lehnert, N. *Inorg. Chem.* **2006**, *45*, 2795. (c) Praneeth, V. K. K.; Haupt, E.; Lehnert, N. *J. Inorg. Biochem.* **2005**, *99*, 940 Erratum: Praneeth, V. K. K.; Haupt, E.; Lehnert, N. *J. Inorg. Biochem.* **2005**, *99*, 1744. (d) Lehnert, N.; Praneeth, V. K. K.; Paulat, F. *J. Comput. Chem.* **2006**, *27*, 1338.
(23) Lim, M. D.; Lorkovic, I. M.; Ford, P. C. *J. Inorg. Biochem.* **2005**, *99*, 151.
(24) (a) Bohle, D. S.; Hung, C.-H. *J. Am. Chem. Soc.* **1995**, *117*, 9584. (b) Choi, I.-K.; Ryan, M. D. *Inorg. Chim. Acta* **1988**, *153*, 25. (c) Liu, Y.; DeSilva, C.; Ryan, M. D. *Inorg. Chim. Acta* **1997**, *258*, 247.
(25) Cullotti, M.; Santagostini, L.; Monzani, E.; Casella, L. *Inorg. Chem.* **2007**, *46*, 8971.

that this issue has not been given enough consideration, in many cases, where it has been simply assumed that the tethering of an N-donor ligand will always lead to coordination to the central metal ion. In order to advance the general design of 6C Fe(II)−heme NO model complexes without the undesirable necessity to add a large excess of the axial ligand (which is unfavorable for reactivity studies),[22b] a detailed evaluation of various tailed porphyrin designs is required. This study represents the first step toward a much needed systematic investigation into the binding properties of tethered N-donor ligands in 6C ferrous heme nitrosyls in solution at room temperature.

Experimental Section

In general, reactions were performed applying inert Schlenk techniques. Preparation and handling of air sensitive materials was carried out under an argon atmosphere in an MBraun glovebox equipped with a circulating purifier (O_2, H_2O < 0.1 ppm). Infrared spectra were obtained from KBr disks or in chloroform solution on a Perkin-Elmer BX spectrometer. Proton magnetic resonance spectra were recorded on a Varian Inova 400 MHz and a Varian Mercury 300 MHz instrument. Electronic absorption spectra were measured using an Analytical Jena Specord 600 instrument. MALDI-TOF mass spectra were obtained on a Micromass TofSpec-2E mass spectrometer whereas LCT-ESI mass spectra were obtained on Micromass LCT Time-of-Flight mass spectrometer. Electron paramagnetic resonance spectra were recorded on a Bruker X-band EMX spectrometer equipped with an Oxford Instruments liquid nitrogen or liquid helium cryostat. EPR spectra were typically obtained on frozen solutions using ∼20 mW microwave power and 100 kHz field modulation with the amplitude set to 1 G. Sample concentrations employed were ∼1 mM.

Crystal structure determination was carried out using a Bruker SMART APEX CCD-based X-ray diffractometer equipped with a low temperature device and a fine focus Mo-target X-ray tube (wavelength = 0.71073 Å) operated at 1500 W power (50 kV, 30 mA). Measurements were taken at 85 K and the detector was placed 5.055 cm from the crystal. The data was processed with SADABS and corrected for absorption.[27b] The structure was solved and refined with the Bruker SHELXTL (ver. 2008/3) software package (cf. Table 1).[27a,c]

Materials. All solvents and reagents were purchased and used as supplied except as follows. Toluene was distilled from sodium under argon. Dried and air free THF and *n*-hexane were obtained after passing through an MBraun solvent purification system. 1-Methylimidazole was vacuum distilled from KOH and degassed via five freeze−pump−thaw cycles. Nitric oxide (Airgas, Royal Oak, MI) was purified by first passing through an ascarite II column (NaOH on silica gel) and then through a cold trap at −80 °C to exclude higher nitrogen oxide impurities. The free base porphyrin ligands H_2TMP-*m*Py and H_2T*o*-F_2PP-C_3IM (ligands **L1** and **L2**, respectively) were synthesized following reported procedures[17,28,29] with some modifications as described in the following. The precursor porphyrins 5,10,15-Tris-(2,4,6-trimethyl-phenyl)-20-(2-amino-phenyl)-porphyrin [$H_2(NH_2)$TMPP] and 5,10,15-Tris-(2,6-difluoro-phenyl)-20-(2-amino-phenyl)-porphyrin [$H_2F_6(NH_2)$TPP] were prepared using reported procedures.[29]

Table 1. Crystallographic Data for Compound [Zn(T*o*-F_2PP-BzIM)]

empirical formula	$C_{56}H_{33}Cl_2F_6N_7OZn$
Formula weight (g/mol)	1070.16
T (K)	85
Space group	Triclinic, $P\bar{1}$
a (Å)	10.522
b (Å)	13.206
c (Å)	19.752
α (deg)	103.955
β (deg)	101.557
γ (deg)	100.116
V (Å^3)	2536.1
Z	2
μ (mm^{-1})	0.659
λ (Å)	0.71073
Collected reflns	54977
Unique reflns	12597
R_{int}	0.0460
GOF	1.075
$R1$ [$I > 2\sigma(I)$]	0.0570
w$R2$ (all data)	0.1770

H_2TMP*m*-Py (Ligand L1). The aminoporphyrin $H_2(NH_2)$TMPP (0.25 g, 0.33 mmol) was dissolved in 6 mL of DMF. To this, 1 mL of *N*,*N*-diethylaniline was added, followed by the addition of a solution of 3-(3′-pyridyl)propionic acid chloride in 3 mL of DMF [prepared in situ by reacting 0.2 g of 3-(3′-pyridyl)propionic acid with 3 mL of $SOCl_2$], and then stirred for 4 h at room temperature. The excess $SOCl_2$ and the solvent were removed under vacuum. The residue obtained was dissolved in CH_2Cl_2 and washed several times with deionized water. The solution was then dried with Na_2SO_4 and the solvent was removed using a rotary evaporator. The desired product was purified using column chromatography (silica, CH_2Cl_2/CH_3OH = 99:1). Yield: 0.20 g, 68%.

UV−vis [nm] in CH_2Cl_2: 418, 514, 545, 590 and 646.

^{1}H NMR (400 MHz, $CDCl_3$): 8.69−8.64 (m, 9H, β-pyrrole (8H) and aminophenyl(1H)); 8.13 (m, 1H, pyridyl); 8.0−7.97 (m, 2H, pyridyl); 7.8 (m, 1H, aminophenyl); 7.48 (m, 1H, pyridyl); 7.26 (s, 6H, mesitylphenyl); 6.9 (m, 1H, aminophenyl); 6.85 (s, 1H, NH-C=O); 6.78 (m, 1H, aminophenyl); 2.61 (s, 6H, para−CH_3); 2.47 (t, 2H, −CH_2−Pyridly); 1.84−1.80 (m, 18H, ortho−CH_3); 1.61 (t, 2H, -**CH_2**−CH_2−Pyridyl); −2.55 (s, 2H, NH pyrrole). MS (MALDI) for $C_{61}H_{56}N_6O$: Calculated: 889, found: 889.

Further Control Experiment. The column purified ligand **L1** was reacted with $Zn(OAc)_2 \cdot 2H_2O$ to yield [Zn(TMP-*m*Py)] in CH_2Cl_2/CH_3OH solution. After shaking with H_2O to remove the unreacted $Zn(OAc)_2$, the solvent was removed under reduced pressure and UV−vis spectra were recorded. The UV−vis spectrum of the product in CH_2Cl_2 shows the Soret band at 430 nm, which corresponds to a five-coordinate Zinc(II)-porphyrin complex.[30] This further proves the presences of the pyridyl linker in ligand **L1**.

[Fe(TMP-*m*Py)(Cl)]. 0.15 g (0.17 mmol) of H_2TMP-*m*Py (**L1**) was stirred in 10 mL of dry and air-free THF. Anhydrous $FeCl_2$ (0.21 g, 1.7 mmol) was then added and the resulting reaction mixture was refluxed at 60 °C under an argon atmosphere for 1 h. The reaction was then stopped and the solvent was removed under reduced pressure. The obtained residue was chromatographed on silica gel using 0.5% methanol in CH_2Cl_2. The metalated porphyrin fraction was collected and the solvent was then removed using a rotary evaporator. The obtained product was dried; yield: 0.11 g, 66%. UV−vis [nm] in CH_2Cl_2: 376, 418, 509, 576, 655, and 692. ^{1}H NMR ($CDCl_3$, 400 MHz): 80 (m, 8H, β-pyrrole).

[Fe(TMP-*m*Py)(NO)] (1). 0.05 g (0.05 mmol) of [Fe(TMP-*m*Py)(Cl)] were placed in a 100 mL Schlenk flask and freshly distilled $CHCl_3$ (8 mL) and CH_3OH (0.5 mL) were added. NO gas was then passed through this solution, and the resulting solution

(26) Collman, J. P.; Yang, Y.; Dey, A.; Decreau, R. A.; Ghosh, S.; Ohta, T.; Solomon, E. I. *Proc. Natl. Acad. Sci. U.S.A.* **2008**, *105*, 15660–15665.
(27) (a) Sheldrick, G. M. *SHELXTL, v. 2008/3*; Bruker Analytical X-ray: Madison, WI, 2008. (b) Sheldrick, G. M. *SADABS, v. 2008/1, Program for Empirical Absorption Correction of Area Detector Data*; University of Gottingen: Gottingen, Germany, 2008. (c) *Saint Plus, v. 7.53a*; Bruker Analytical X-ray: Madison, WI, 2008.
(28) (a) Collman, J. P.; Zhong, M.; Wang, Z.; Rapta, M. *Org. Lett.* **1999**, *1*, 2121–2124.
(29) Collman, J. P.; Brauman, J. I.; Doxee, K. M.; Halbert, T. R.; Bunnenberg, E.; Linder, R. E.; LaMar, G. N.; Gaudio, J. D.; Lang, G.; Spartalin, K. *J. Am. Chem. Soc.* **1980**, *102*, 4182–4192.
(30) Lin, C.-L.; Fang, M.-Y.; Cheng, S.-H. *J. Electroanal. Chem.* **2002**, *531*, 155–162.

was stirred for one hour. *n*-Hexane (10 mL) was slowly added to the reaction mixture, which was then stored in a freezer (−22 °C) for 3 days. The resulting precipitate was filtered off using a fine pore Schlenk filter funnel. The yield of the product obtain was very low, 11 mg (22%), and contained some impurities. FT-IR [cm^{-1}]: ν(NO) = 1694.

H_2T*o*-F_2PP-C_3IM (Ligand L2). 4-(*N*-Imidazolyl)butyric acid hydrobromide[29] (0.18 g, 0.4 mmol) was ground to a fine powder and stirred in 5 mL of dry and air-free CH_2Cl_2. The solution was brought to reflux under argon and 35 mg (0.3 mmol) $SOCl_2$ was then added. The solution was stirred at reflux under an argon atmosphere. After 30 min, the excess $SOCl_2$ and CH_2Cl_2 were removed under vacuum and a solution of $H_2F_6(NH_2)$TPP (0.1 g, 0.135 mmol) in 5 mL of CH_2Cl_2 was added and the resulting green solution was stirred for 1 h under argon at room temperature. The reaction was then stopped by pouring the solution into 20 mL of CH_2Cl_2 and successive washing with 2 × 20 mL of Na_2CO_3, and 3 × 20 mL of water, and then drying over Na_2SO_4. The solvent was removed under reduced pressure and the residue obtained was column purified on silica gel (CH_2Cl_2/CH_3OH = 95:5) to give the desired C_3 imidazole linked porphyrin ligand H_2T*o*-F_2PP-C_3IM. Yield: 0.045 g, 38%.

^{1}H NMR (300 MHz, *d*-acetone): 9.15−8.80 (m, 8H, β-pyrrole); 8.55 (d, 1H, aminophenyl); 8.44 (s, 1H, amide); 8.11 (dd, 1H, aminophenyl); 8.05−7.95 (m, 3H, *para* fluorophenyl); 7.86 (t, 1H, aminophenyl); 7.65−7.45 (m, 7H, *meta* fluorophenyl (6H) and aminophenyl (1H)); 7.02 (s, 1H, imidazole); 6.44 (s, 1H, imidazole); 6.42 (s, 1H, imidazole); 3.45 (t, 2H, C_3H_6 tether); 1.58 (t, 2H, C_3H_6 tether); 0.90 (m, 2H, C_3H_6 tether); −2.69 (s, 2H, pyrrole NH). See Figure S15 (Supporting Information).

UV−vis [nm] in CH_2Cl_2: 415, 509, 543, 587, and 642. MS (LCT-ESI) for $C_{51}H_{33}N_7F_6O$: Calculated: 873.8, found: 874.

Further Control Experiment. The column purified ligand **L2** was reacted with $Zn(OAc)_2 \cdot 2H_2O$ to yield [Zn(T*o*-F_2PP-C_3IM)] in a CH_2Cl_2/CH_3OH solution. After shaking with H_2O to remove the unreacted $Zn(OAc)_2$, the solvent was removed under reduced pressure and UV−vis spectra were recorded. The UV−vis spectrum of the product in CH_2Cl_2 shows the Soret band at 427 nm, which is in accordance with similar values observed for five-coordinate Zinc(II)-porphyrin complexes[30] (substituted tetraphenylporphyrins with electron withdrawing or donating groups attached to the phenyl rings). This further proves the presence of the imidazolyl linker in ligand **L2**.

MS (LCT-ESI) for $ZnC_{51}H_{31}N_7F_6O$: Calculated: 935.1, found: 936.1. ^{1}H NMR spectra of the zinc metalated complex [Zn(T*o*-F_2PP-C_3IM)] reveal a shift of the imidazole proton peaks into the porphyrin aromatic region. This is most likely due to an exposure of the imidazole unit to the aromatic porphyrin ring current upon binding to the zinc center.

[Fe(T*o*-F_2PP-C_3IM)(Cl)]. 0.03 g (0.034 mmol) of H_2T*o*-F_2PP-C_3IM were stirred in 8 mL of dry and air free THF. Anhydrous $FeCl_2$ (0.043 g, 0.34 mmol) was then added and the resulting reaction mixture was refluxed under an argon atmosphere for 1 h. The reaction was then stopped and the solvent was removed under reduced pressure. The obtained residue was chromatographed on silica gel using 3% methanol in CH_2Cl_2. The metalated porphyrin fraction was collected, and the solvent was then removed using a rotary evaporator. Yield: 0.023 g, 70%.

UV−vis [nm] in CH_2Cl_2: 350, 415, 510, 557, and 642. FT-IR in KBr [cm^{-1}]: $\nu_{C=O}$ = 1700.

[Fe(T*o*-F_2PP-C_3IM)(NO)] (2). To a solution of [Fe(T*o*-F_2PP-C_3IM)(Cl)] (0.02 g, 0.02 mmol) in 10 mL of freshly distilled $CHCl_3$ and 0.5 mL of CH_3OH was added excess nitric oxide and the resulting solution was stirred for one hour. *n*-Hexane (15 mL) was slowly added to the reaction mixture, which was then stored in a freezer (−20 °C) for 1 day. The resulting precipitate was filtered off and the obtained compound was stored inside a glovebox. The IR spectrum shows the NO stretching band at 1686 cm^{-1}, indicative of the formation of **2**.

Yield: 0.010 g, 52%: FT-IR in KBr [cm^{-1}]: ν(NO) = 1686.

To test whether complex **2** is really a monomer, we performed dilution experiments where the concentration was lowered to an intensity of 0.2 absorbance units. No shift of the Soret band was observed, indicating that the complex does not correspond to a dimer (oligomer) where two complexes (or more) share linkers.

***N*-(3-Methoxycarbonyl)benzylimidazole.** Imidazole (3.8 g, 55.8 mmol) and methyl 3-bromomethyl-benzoate (3.1 g, 13.5 mmol) were combined in 4 mL of DMF. The resulting faint yellow solution was stirred at room temperature for 20 h. Upon completion, the reaction was diluted with 60 mL of water and extracted 3× with a total of 120 mL CH_2Cl_2. The organic layer was collected and extracted 3× with a total of 150 mL of a 10% HCl solution. The acidic solution was then alkalized with triethylamine to pH = 10, extracted 3× with a total of 210 mL ethyl acetate followed by drying over Na_2SO_4. Rotary evaporation of the solvent yielded a faint-yellow oil in quantitative amounts. ^{1}H NMR (300 MHz, $CDCl_3$): 7.99 (d, 1H), 7.88 (s, 1H), 7.56 (s, 1H), 7.41 (t, 1H), 7.32 (d, 1H), 7.01 (s, 1H), 6.89 (s, 1H), 5.16 (s, 2H), 3.91 (s, 3H).

α-Imidazolyl-*m*-toluic Acid Hydrochloride. *N*-(3-Methoxycarbonyl)benzylimidazole (3.0 g, 13.9 mmol) was dissolved in 27 mL of conc. HCl and brought to reflux while stirring for 2 h. The HCl was then removed on a vacuum line and the resulting off-white solid was dried under vacuum overnight. The next day, the product was washed with hot acetonitrile and filtered to remove a yellow-colored impurity. The resulting white solid was again dried under vacuum. Yield: 2.0 g, 61%. ^{1}H NMR (300 MHz, CD_3OD): 9.13 (s, 1H), 8.06 (s, 1H), 8.05 (s, 1H), 7.66 (d, 1H), 7.60 (s, 1H), 7.57 (m, 2H), 5.56 (s, 2H).

H_2T*o*-F_2PP-BzIM (Ligand L4). (Adapted from ref 31). α-Imidazolyl-*m*-toluic acid hydrochloride (0.1 g, 0.42 mmol) and an excess thionyl chloride (0.1 mL, freshly distilled under Ar) in methylene chloride (2 mL) were refluxed under an argon atmosphere. After 1 h the solution became clear. The excess $SOCl_2$ and CH_2Cl_2 were removed in vacuo to yield crude α-imidazolyl-*m*-toluic acid chloride as an off-white solid. In a separate flask, a solution of the porphyrin $H_2F_6(NH_2)$TPP (0.088 g, 0.119 mmol) in 15 mL dry and air-free CH_2Cl_2 was stirred. To this stirred solution a suspension of α-imidazolyl-*m*-toluic acid chloride (from above) in CH_2Cl_2 (4 mL) was slowly added in small portions under an argon atmosphere at room temperature (color changed to green). The reaction was monitored by TLC (silica, CH_2Cl_2) until the only visible porphyrin remained at the baseline. The solution was diluted with 100 mL CH_2Cl_2 and shaken with 40 mL saturated $NaHCO_3$, washed 3× with 50 mL water, and dried with sodium sulfate. Rotary evaporation of the solvent yielded a purple solid. The product was purified on silica gel using column chromatography with 5% MeOH in CH_2Cl_2 as eluent. Yield: 100 mg, 92%. UV−vis [nm] in CH_2Cl_2: 416, 509, 542, 586, and 640. ^{1}H NMR (300 MHz, CD_2Cl_2): 9.0−9.85 (m, 9H, β-pyrrole (8H) and aminophenyl (1H)); 8.22 (dd, 1H, benzyl); 7.95−7.80 (m, 4H, *para* fluorophenyl (3H) and aminopheyl (1H)); 7.65 (m, 1H, aminophenyl); 7.50−7.37 (m, 8H, *meta* fluorophenyl (6H) and benzyl (2H)); 6.78 (s, 1H, NH−C=O); 6.47−6.38 (m, 2H, benzyl (1H) and aminophenyl (1H)); 6.33 (m, 1H, imidazolyl); 6.19 (s, 1H, imidazolyl); 6.07 (S, 1H, imidazolyl); 3.88 (s, 2H, $-CH_2$-benzyl); −2.75 (s, 2H, NH pyrrole). See Figure S16 (Supporting Information). MS (MALDI) for $C_{54}H_{34}N_7F_6O$; Calculated: 922, found: 922.

[Fe(T*o*-F_2PP-BzIM)(Cl)]. 0.03 g of H_2T*o*-F_2PP-BzIM were stirred in 10 mL of dry and air free THF. Anhydrous $FeCl_2$ (0.039 g) was then added, and the resulting reaction mixture was refluxed under an argon atmosphere for 1 h. The reaction was then stopped and the solvent was removed under reduced pressure. The obtained residue was chromatographed on silica gel using 5% methanol in CH_2Cl_2. The metalated porphyrin fraction (slowest moving) was collected, and the solvent was removed using a rotary evaporator. The product obtained was finally dried. Yield: 27 mg, 82%. UV−vis

(31) Young, R.; Chang, C. K. *J. Am. Chem. Soc.* **1985**, *107*, 898–909.

[nm] in CH_2Cl_2: 337, 413, 577, and 650. FT-IR in KBr [cm^{-1}]: $\nu_{C=O} = 1684$. MS (LCT-ESI) calculated: 975 (M-Cl), found: 975.

[Zn(T*o*-F_2PP-BzBr)]. The same procedure as for [Zn(T*o*-F_2PP-BzIM)] was used, except that T*o*-F_2PP-BzBr was synthesized with an acid chloride made from $SOCl_2$ and methyl 3-bromomethylbenzoate to yield T*o*-F_2PP-BzBr where the imidazole is lacking to prevent binding of the linker to zinc. UV−vis (nm) in CH_2Cl_2: 416, 510, 543, 585.

[Zn(T*o*-F_2PP-BzIM)]. 0.026 g of H_2T*o*-F_2PP-BzIM were stirred in 10 mL of dry and air free CH_2Cl_2. $Zn(OAc)_2$ dihydrate (0.250 g) was then added along with 1 mL MeOH, and the resulting reaction mixture was stirred at room temperature for 1.5 h. The color of the solution changed from deep red to magenta. The reaction was washed 3× with water, and dried with sodium sulfate. Rotary evaporation of the solvent yielded a magenta colored solid. Purification on a silica column eluted with CH_2Cl_2 yielded a pure magenta solid (23.8 mg, 84%). UV−vis (nm) in CH_2Cl_2: 427, 559, 598.

Further Control for IM Binding. The UV−vis spectrum of [Zn(T*o*-F_2PP-BzIM)] in CH_2Cl_2 shows the Soret band at 427 nm, which is in accordance with similar values observed for five-coordinate Zinc(II)-porphyrin complexes.[30] In comparison, the analogous complex [Zn(T*o*-F_2PP-BzBr)] which lacks the IM ligand shows the Soret band at 416 nm. See Results and Discussion 4.

Crystallization of [Zn(T*o*-F_2PP-BzIM)]. [Zn(T*o*-F_2PP-BzIM)] (18 mg) was dissolved with two 5S in 2 mL of 10% chlorobenzene in CH_2Cl_2 in a Schlenk tube which was cooled to 4 °C. This tube was then connected via glass joints to a Schlenk flask with *n*-hexane stirred at 35 °C. After four days in the dark, enough *n*-hexane had diffused over to obtain crystals suitable for crystallographic analysis.

[Fe(T*o*-F_2PP-BzIM)(NO)] (4). To a solution of the iron(III)-porphyrin, [Fe(T*o*-F_2PP-BzIM)(Cl)] (0.02 g, 0.02 mmol) in 10 mL of freshly distilled $CHCl_3$ and CH_3OH (0.5 mL), excess nitric oxide was added, and the resulting solution was stirred for one hour under an NO atmosphere. *n*-Hexane (15 mL) was slowly added to the reaction mixture, which was then stored in a freezer (−20 °C) for 1 day. The resulting precipitate was filtered off using a fine pore Schlenk filter funnel, and the obtained compound was stored inside a glovebox. The IR spectrum shows the NO stretching band at 1644 cm^{-1}, indicative of the formation of **4**. Yield: 14 mg, 70%.

H_2T*o*-F_2PP-C_4IM (L3), [Fe(T*o*-F_2PP-C_4IM)(Cl)], and [Fe(T*o*-F_2PP-C_4IM)(NO)] (3). The preparation of H_2T*o*-F_2PP-C_4IM was performed by the same method as described for H_2T*o*-F_2PP-BzIM, but using 5-bromopentanoic acid in place of α-bromotoluic acid to build the alkyl chain. ^{1}H NMR (300 MHz, *d*-acetone): 9.10−8.80 (m, 8H, *β*-pyrrole); 8.54 (d, 1H, aminophenyl); 8.41 (s, 1H, amide); 8.09 (dd, 1H, aminophenyl); 8.05−7.90 (m, 3H, *para* fluorophenyl); 7.86 (t, 1H, aminophenyl); 7.65−7.45 (m, 7H, *meta* fluorophenyl (6H) and aminophenyl (1H)); 7.04 (s, 1H, imidazole); 6.52 (s, 1H, imidazole); 6.44 (s, 1H, imidazole); 3.30 (t, 2H, C_4H_8 tether); 1.44 (t, 2H, C_4H_8 tether); 1.08 (m, 2H, C_4H_8 tether); 0.90 (m, 2H, C_4H_8 tether); −2.72 (s, 2H, pyrrole NH). See Figure S15 (Supporting Information). UV−vis [nm] in CH_2Cl_2: 414, 510, 541, 586, and 641. MS (LCT-ESI) for $C_{52}H_{35}N_7F_6O$: Calculated: 887.9, found: 888.

Iron insertion into H_2T*o*-F_2PP-C_4IM and the synthesis of [Fe(T*o*-F_2PP-C_4IM)(NO)] (**3**) also followed the same procedures as described for **4**.

[Fe(T*o*-F_2PP-C_4IM)(Cl)]. UV−vis [nm] in CH_2Cl_2: 342, 414, 503, 574, and 650.

FT-IR in KBr [cm^{-1}]: $\nu_{C=O} = 1719$.

Results and Discussion

1. Spectroscopic Distinction between 5C and 6C Ferrous Heme Nitrosyls. To investigate the formation of a six-coordinate (6C) ferrous heme nitrosyl in solution according to the equation:

$$Fe^{II}(NO) + IM \rightleftarrows Fe^{II}(NO)(IM) \quad (IM = \text{imidazole}) \qquad (2)$$

it is most important to perform room temperature measurements. This is because the binding of axial ligands is entropically favored at low temperature, due to the temperature dependent component of the Gibbs−Helmholtz equation. Methods of assessing the strength of the N-donor coordination to the heme center which require low temperatures are thus not a definitive means of determining the room temperature behavior of these systems. They can, however, still provide a means by which to compare different systems. In this study, we use room temperature UV−vis and IR spectroscopy, coupled to low temperature EPR spectroscopy, to access the binding properties of our tethered N-donor ligands. In the case of UV−vis spectroscopy, the Soret band maximum shows a direct correlation with the coordination number of the iron center. Five-coordinate (5C) heme nitrosyls show Soret band positions of about 405 nm. With IM bound, the Soret maximum shifts to 426 nm and the complex is 6C. A corresponding, direct correlation is also observed between the N−O stretching mode ν(N−O) and the coordination number: 5C complexes exhibit ν(N−O) around 1675−1700 cm^{-1}, whereas in 6C species, ν(N−O) drops to ∼1630 cm^{-1} in the presence of IM. Additionally, low temperature EPR spectroscopy can be an effective probe of N-donor coordination to ferrous heme nitrosyls.[32] Species which are 5C in solution show g values of 2.10, 2.06, and 2.01 as well as a three line hyperfine splitting on g(min). On the other hand, 6C ferrous heme nitrosyls with axial N-donor coordination exhibit smaller g values around 2.08, 2.00, and 1.97 as well as a distinctive nine line hyperfine splitting observed on g(mid). Since EPR spectroscopy requires low (at least liquid nitrogen) temperatures, which, as discussed above, entropically favors the coordination of the axial N-donor ligand, it can be expected that N-donor binding at room temperature will generally be somewhat weaker than determined from EPR. Finally, Raman spectroscopy could potentially be applied to ferrous heme nitrosyls to characterize the strength of the Fe−NO bond via measurement of the ν(Fe−NO) stretch. However, photodecomposition is a serious problem in this case when these complexes are exposed to the laser radiation required for Raman measurements.

2. Application of Pyridine versus Imidazole as a Proximal Ligand. In this study, "tailed" porphyrins with covalently attached imidazole (IM) or pyridine (Py) ligands have been investigated with the specific aim of determining the requirements for the generation of truly 6C ferrous heme nitrosyl model complexes in solution at room temperature. These tailed porphyrins are preferred over the use of excess free IM, because they offer (a) control over the molar stoichiometry, (b) defined structures of the complexes, and (c) prevention of side reactions due to the presence of free axial ligand.[33] The first consideration involved in designing a 6C ferrous heme nitrosyl complex is the choice of the axial N-donor ligand. We started this investigation with a model complex based on H_2TMP (TMP = tetramesitylporphyrin) with a covalently attached Py (ligand **L1** in Figure 1). Reaction of the ferric precursor with NO gas in the presence of a small amount of methanol generates the corresponding ferrous heme nitrosyl complex. However, the compound obtained, [Fe(TMP-*m*Py)(NO)] (**1**), forms only a 5C complex in solution, that is, the Py does not bind to the

(32) Lehnert, N. EPR and Low-Temperature Magnetic Circular Dichroism Spectroscopy of Ferrous Heme Nitrosyls. In *The Smallest Biomolecules: Diatomics and their Interactions with Heme Proteins*; Ghosh, A., Ed.; Elsevier: Amsterdam, 2008.

(33) Wasser, I. M.; Huang, H.; Moënne-Loccoz, P.; Karlin, K. D. *J. Am. Chem. Soc.,* **2005**, *127*, 3310–3320.

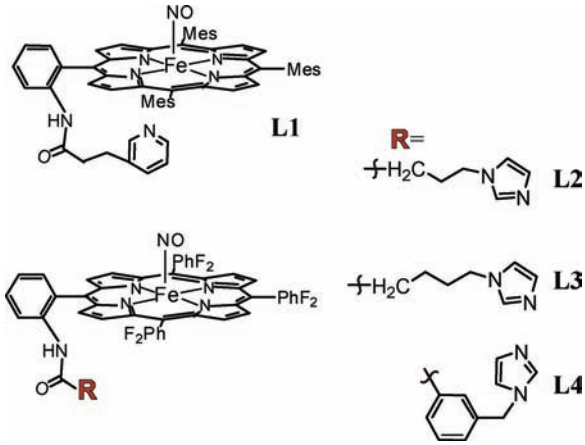

Figure 1. Drawings of the iron(II)-porphyrin NO complexes with covalently attached N-donor ligands employed in this study.

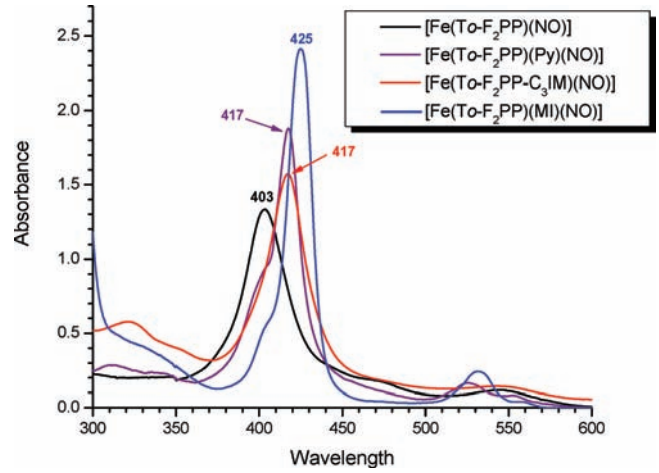

Figure 2. Electronic absorption spectrum of [Fe(T*o*-F_2PP-C_3IM)(NO)] (**2**, red) in comparison to 5C [Fe(T*o*-F_2PP)(NO)] (black), and the 6C complexes [Fe(T*o*-F_2PP)(MI)(NO)] (blue, MI = free 1-methylimidazole) and [Fe(T*o*-F_2PP)(Py)(NO)] (purple, Py = free pyridine). Spectra were recorded in CH_2Cl_2 or toluene solution at room temperature.

Fe(II)−NO center. This is evident from the low-temperature (LT) EPR data of **1** in Figure S1 (Supporting Information), which show a characteristic 5C spectrum with g values of 2.10, 2.04, and 2.01 as well as a three line ^{14}N hyperfine pattern on the smallest g value, *g*(min).[32] The room temperature FT-IR spectrum of **1** exhibits ν(NO) at 1694 cm^{-1} (Figure S3, Supporting Information), in agreement with values of other 5C complexes such as [Fe(TPP)NO] and [Fe(TMP)NO] at 1697 cm^{-1} and 1676 cm^{-1}, respectively.[34] Hence, the stereotype that simple attachment of an N-donor ligand to the porphyrin core should promote its coordination to the iron center is misleading. These results, however, agree with the very weak binding affinity of Py to Fe(II)−NO previously observed for different types of tetraphenylporphyrin ligands.[22b,35] In these studies it was found that binding constants of free pyridine are only in the range of 3 M^{-1} to 7 M^{-1} depending on the nature of the porphyrin ligand employed. During our axial ligation titration experiments reported in ref 22b, we found that, in general, the binding constants for 1-methylimidazole (MI) are one order of magnitude larger (typically between 20−40 M^{-1}) than those seen for Py. Therefore, Py is not a suitable axial ligand for 6C ferrous heme nitrosyls and IM-type ligands are preferred due to their larger binding constants. However, even in the case of IM-type N-donors, the equilibrium between the 5C Fe(II)−NO complex and the 6C (IM)N−Fe(II)−NO adduct shown in eq 2 disfavors the formation of the 6C species. This is because the presence of 1 equiv of an N-donor ligand with a typical binding constant (K_{eq}) < 50 M^{-1} will not lead to the formation of significant amounts of the 6C species in solution due to the equilibrium strongly favoring the reactant side.[36] In this case, the strong *σ-trans* effect of NO prevents binding of the axial ligand.[22b,37] The formation of 6C Fe(II)−NO complexes in the absence of excess N-donor ligands thus presents a significant challenge.

Importantly, our previous studies have also shown that a further improvement of the axial ligand binding constant can be achieved by using the combination of a weakly electron-withdrawing tetra(*ortho*-difluorophenyl)porphyrin ligand (H_2T*o*-F_2PP) and free imidazole. In this case, a dramatic increase of the IM binding constant to 2055 M^{-1} is observed.[22b] On the other hand, the application of the porphyrin H_2T*o*-F_2PP hardly affects the properties of the Fe(II)−NO subunit as indicated by the ν(N−O) stretching mode, which is only 6 cm^{-1} lower in [Fe(T*o*-F_2PP)(MI)(NO)] compared to [Fe(TPP)(MI)(NO)].[22b] The binding constant of free MI to these fluorinated porphyrins therefore shows a nearly 300-fold increase over the pyridine derivative of the same system. In conclusion, the first requirements for the design of a truely 6C ferrous heme nitrosyl in solution are to (a) use IM as the N-donor ligand and (b) utilize *ortho* difluorophenyl substituted TPP or other slightly electron poor porphyrins. This provides a good basis in order to overcome the strong *σ trans* effect of NO and obtain a 6C complex in solution at room temperature in the presence of only 1 equiv of the N-donor ligand. Based on these results, we decided to use IM ligands tethered to the fluorinated porphyrin T*o*-F_2PP for our further studies. In the next step, the linker arm which covalently links the N-donor ligand to the porphyrin core needs to be optimized.

3. Imidazole Ligation with Alkyl Chain Tethers. In light of the above-mentioned results, we synthesized ligand **L2** in Figure 1 employing a C_3 alkyl chain-linked IM attached to a fluoro-substituted tetraphenylporphyrin. The UV−vis spectrum of the obtained ferrous heme nitrosyl, [Fe(T*o*-F_2PP-C_3IM)(NO)] (**2**), exhibits the Soret band maximum at 417 nm as shown in Figure 2 (red curve). Interestingly, this is intermediate between the Soret position of the 5C complexes [Fe(TPP*)(NO)] (TPP* = tetraphenylporphyrin type ligand) at ∼405 nm, and the IM coordinated (6C) species [Fe(TPP*)(IM)(NO)] at ∼425 nm (cf. Figure 2). To test whether the 417 nm Soret band of **2** corresponds to weak binding of the axial ligand, we recorded the UV−vis spectrum of the 6C Py complex [Fe(T*o*-F_2PP)(Py)(NO)] for comparison, because in this case, it is known that the Fe(II)−Py interaction is very weak.[22b,37] As shown in Figure 2 (purple curve), the spectra of **2** and [Fe(T*o*-F_2PP)(Py)(NO)] show good agreement. Importantly, the lack of a shoulder between 400 and 407 nm and around 470 nm for **2** confirms that no (or very little) 5C species is present in solution. In addition to UV−vis data, FT-IR spectroscopy can also be used to probe the coordination number of ferrous heme nitrosyls through the N−O stretching mode ν(N−O), as

(34) Scheidt, W. R.; Ellison, M. K. *Acc. Chem. Res.* **1999**, *32*, 350–359.
(35) Choi, I.-K.; Ryan, M. D. *Inorg. Chim. Acta* **1988**, *153*, 25–30.
(36) (a) Hoshino, M.; Ozawa, K.; Seki, H.; Ford, P. C. *J. Am. Chem. Soc.* **1993**, *115*, 9568–9575. (b) Traylor, T. G.; Sharma, V. S. *Biochemistry* **1992**, *31*, 2847–2849.
(37) Wyllie, G. R. A.; Schulz, C. E.; Scheidt, W. R. *Inorg. Chem.* **2003**, *42*, 5722–5734.

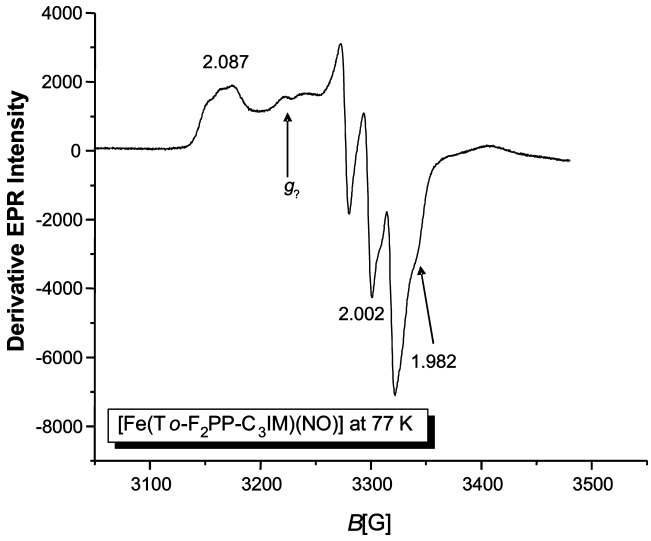

Figure 3. EPR spectrum of [Fe(T*o*-F_2PP-C_3IM)(NO)] (**2**) in DMSO at liquid nitrogen temperature. A simulation of these data is shown in Figure S6 (Supporting Information). The additional signal $g_?$ is typically observed for 6C ferrous heme nitrosyls in both proteins and model complexes. See text for a detailed explanation and relevant references.

mentioned above. Interestingly, as elaborated below, the magnitude of the downshift of ν(N−O) is a direct function of the Fe−N(IM) bond strength, mediated by the *trans* interaction between the N-donor ligand and NO. The FT-IR spectrum of **2**, taken at room temperature in a KBr disk, shows a broad intense band at 1686 cm^{-1} (Figure S4, Supporting Information), which is assigned to the ν(N−O) stretch. This energy of ν(N−O) is not far off from values of known 5C complexes such as [Fe(TPP)NO] or [Fe(TMP)NO] (vide supra) and thus indicates a very weak covalent interaction between IM and the heme center.[22b]

More insight is available from EPR spectroscopy. The EPR spectrum of **2**, shown in Figure 3, clearly resemble the spectra of other 6C complexes.[32] Hyperfine splittings observed within these spectra can reveal a great deal of information about the coordination environment of the central iron in heme nitrosyls and has traditionally been used to distinguish between 5C and 6C complexes.[32] This information manifests itself not only in the number of hyperfine lines observed, but also in the particular g value which exhibits the well-resolved hyperfine splittings. In the case of 5C ferrous heme nitrosyl complexes such as [Fe(TPP)(NO)], three g values are observed at 2.10, 2.06, and 2.01. The smallest of these, g(min), shows clear three line hyperfine splittings due to the interaction of the nuclear spin ($I = 1$) of ^{14}N(O) with the unpaired electron of the Fe(II)−NO unit. The fact that the well-resolved hyperfine splittings are seen on g(min) indicates that the principal axis of this g-value is aligned closest to the Fe−N(O) axis.[22a,32] For 6C complexes with NO and IM in the axial positions, the g shifts are smaller with g values of about 2.07, 2.00, and 1.97.[32] In addition, the three hyperfine lines are further split, due to the presence of ^{14}N of IM, to give a nine line hyperfine pattern, which is now observed on g(mid) because of a rotation of the g tensor.[22a,32] The spectrum of **2** at 77 K, shown in Figure 3, exhibits strong ^{14}N hyperfine lines of NO on g(mid), and the *g* values are obtained at 2.09, 2.00, and 1.98. In the lq. helium spectrum additional, small, unresolved hyperfine splittings due to the axial IM ligand seem to be present on g(mid). The obtained g values and the presence of hyperfine splittings on g(mid) are generally indicative that **2** is a 6C complex in agreement with the UV−vis result. However, the lack of clear nine-line hyperfine splittings of this signal indicates very weak binding of IM to iron as is also reflected by the large value of ν(N−O). This is further supported by the small hyperfine coupling constant of the IM nitrogen estimated at around 2.0 MHz for **2** compared to 16−19 MHz for N-donor ligands in known 6C complexes.[38] EPR spectra are ideally suited for assessing the Fe−IM bond strength as the covalency of the Fe−IM bond directly correlates with the amount of spin density transferred from the Fe(II)−NO unit to the N-donor atom of IM.[22b] The spin density present on the IM nitrogen atom then correlates with the contact shift, and hence, the magnitude of the ^{14}N(IM) hyperfine coupling constant. In this sense, weak bonding results in minimal transfer of spin density between Fe and IM, resulting in almost no contact shift and a small hyperfine coupling constant, likely dominated by the dipolar contribution. A stronger Fe−IM bond will manifest itself in an increase in contact shift, leading to a larger hyperfine coupling constant, and thus a cleaner resolution of hyperfine lines on g(mid).

The EPR spectrum of **2** in Figure 3 also shows a fourth g value which is typically observed for 6C ferrous heme nitrosyl complexes in both proteins and model systems.[32] This signal is usually referred to as $g_?$ and is clearly identified in the case of both **2** and **3**. Interestingly, this additional signal seems to be absent in 5C heme nitrosyls. The origin of $g_?$ has been a matter of extended discussion in the literature.[39−41] It has been proposed that this signal arises from a second conformation of the complex where the relative orientation of NO, with respect to the IM plane, has shifted.[32] This is consistent with the observation that crystal structures of 6C model complexes usually show disorder of the NO ligand, giving rise to two major conformations.[22b,37,42] To rule out binding of the solvent DMSO in the case of **2** and **3**, the EPR spectrum of the 5C complex [Fe(TPP)(NO)] was recorded in a DMSO/toluene mixture (1:1) (cf. Figure S8, Supporting Information). These data resemble more closely the typical 5C spectrum of this compound in pure toluene. Additionally, the UV−vis spectrum of [Fe(TPP)(NO)] in DMSO shows the Soret band at 409 nm, indicative of a 5C complex. Therefore, binding of DMSO to complex **2** can be ruled out in the EPR experiments. Based on all available spectroscopic results, it can be concluded that complex **2** is 6C in solution at room temperature, but that the interaction of the C_3 imidazole arm with the Fe(II)-NO center is weak.

There are two possible reasons for the weak binding of the C_3 imidazole linker in ligand **L2**: (a) the alkyl chain of the 'C_3' linker is too short to allow for a good interaction of IM with iron(II), or (b) the dynamic motion of the phenyl rings leads to a constant alkyl chain motion in solution, which prevents effective binding of the imidazole ligand to iron(II) (see Results and Discussion 4). In order to determine the influence of the alkyl chain length on the binding properties of the linked IM, we prepared a corresponding complex where the length of the

(38) (a) Kon, H.; Kataoka, N. *Biochemistry* **1969**, *8*, 4757–4762. (b) Wayland, B. B.; Olson, L. W. *J. Am. Chem. Soc.* **1974**, *96*, 6037–6041.
(39) Morse, R. H.; Chan, S. I. *J. Biol. Chem.* **1980**, *255*, 7876–7882.
(40) Hüttermann, J.; Burgand, C.; Kappl, R. *J. Chem. Soc. Faraday Trans.* **1994**, *90*, 3077–3087.
(41) Tyryshkin, A. M.; Dikanov, S. A.; Reijerse, E. J.; Burgard, C.; Huttermann, J. *J. Am. Chem. Soc.* **1999**, *121*, 3396–3406.
(42) (a) Silvernail, N. J.; Pavlik, J. W.; Noll, B. C.; Schulz, C. E.; Scheidt, W. R. *Inorg. Chem.,* **2008**, *47*, 912–920. (b) Silvernail, N. J.; Barabanschikov, A.; Sage, J. T.; Noll, B. C.; Scheidt, W. R. *J. Am. Chem. Soc.* **2009**, *131*, 2131–2140.

alkyl chain is increased by one CH_2 unit (ligand **L3** in Figure 1). Importantly, the UV−vis and EPR spectra of this complex, [Fe(T*o*-F_2PP-C_4IM)(NO)] (**3**) (cf. Figures S9 and S10, Supporting Information), again show weak binding of the IM linker to the iron(II) center with a Soret maximum at 415 nm. In particular, the absorption spectrum in Figure S9 (Supporting Information) is indicative of the presence of a small amount of 5C complex in solution at room temperature, as evidenced by a very pronounced shoulder at 405 nm. This counterintuitive result shows that an increase of the alkyl chain length from "C_3" to "C_4" actually has a negative effect, i.e. *the increase in length or flexibility of the linker slightly decreases the binding constant of the tethered IM ligand to iron(II)*. This is most likely due to a loss of entropy of internal rotation as discussed before for tailed Zn-porphyrins.[43] Here, entropy loss was observed for each additional CH_2 unit added to the alkyl tethers within these systems. EPR spectra of complex **3** are in agreement with this conclusion and show g values at 2.07, 1.99, and 1.97, which are almost identical to those for **2**, indicating that an increase in tether length does not increase the Fe−IM covalency, and hence, bond strength (see Figures S6 and S11 in the Supporting Information). No 5C species is observed in the EPR spectra of **3**, but this is likely due to a slight increase in the IM binding constant at low temperature compared to the room temperature UV−vis data (see Results and Discussion 1).

4. Application of the More Rigid Benzyl Linker. Our systematic studies on IM binding to ferrous heme nitrosyls presented above therefore show that pyridyl donors and C_3−IM or C_4−IM tethers (**L1**−**L3**) are poor designs for 6C ferrous heme nitrosyls in solution. Because of the poor binding seen for both **2** and **3**, it can be inferred that the length of the tether is not as important as its other structural properties.

On the basis of this result, we decided to explore whether a more rigid (less floppy) linker with a larger mass could change the dynamics of the linker motion and facilitate a 6C complex. For this purpose, a benzyl group was incorporated into the linker, leading to ligand H_2T*o*-F_2PP-BzIM (**L4**) in Figure 1. From the literature, work of Collman and co-workers has presented evidence that a similar linker could indeed allow for the formation of a 6C species in solution, although the room temperature characterization of the corresponding complex was incomplete.[26] Ligand **L4** was prepared and crystallographically characterized as the corresponding Zn complex. The crystal structure of this compound is shown in Figure 4 and important structural parameters are listed in Tables 2 and S1−S5 (Supporting Information). The obtained bond distances and angles reveal very little strain within the tether. The only sizable perturbation from expected values is seen in the CNC angle of 129.1° for the amide linkage. This value is several degrees larger than expected for an idealized system but only slightly larger than amide CNC angles in other corresponding zinc porphyrin compounds. The zinc complex of α,α,α,α-Tetra-(2-[3,4-dimethoxyphenyl]-acetamidophenyl)porphyrin, for example, exhibits an amide CNC angle of 128°.[44] The zinc within the porphyrin center of the **L4** complex is clearly displaced toward the IM tether by about 0.5 Å from the porphyrin plane. The Zn−N(imidazole) bond distance is 2.079 Å. The average Zn−N(porphyrin) bond distance is 2.077 Å, which is slightly longer than the average bond length of 2.050 Å observed in four-coordinate [Zn(TPP)].[45] On the other hand, this value is in agreement with the 5C complexes [Zn(TPP)(3-APy)] (3-APy = 3-aminopyridine) and [Zn(OPP)(3-APy)] (OPP^{2-} = octaphenylporphyrin) where average Zn−N(porphyrin) bond lengths of 2.080 Å and 2.075 Å have been determined, respectively.[46] The structure is well ordered with the single exception of the phenyl ring located opposite to the tether position. Two possible orientations are seen in the crystal structure where the phenyl ring rotates slightly off the perpendicular geometry with respect to the porphyrin plane, in both possible directions. The porphyrin ligand itself shows very little distortion and appears only to be slightly domed toward the IM ligand. The UV−vis adsorption data obtained for the complex [Zn(T*o*-F_2PP-BzIM)] show the Soret band at 427 nm. This is in agreement with know 5C Zn(II)−porphyrin complexes.[30] The analogous complex [Zn(T*o*-F_2PP-BzBr)], where IM has been replaced by a noncoordinating bromine, shows typical UV−vis absorption features of four-coordinate (4C) Zn(II)−porphyrin complexes where the Soret band is observed at 416 nm (cf. Figure 5). Due to these characteristic absorption features, zinc-metalated porphyrin species can be a useful tool to determine the coordination environment of tethered porphyrin systems, and in particular, to probe for the presence and binding properties of an attached linker.

Next, the ferrous heme nitrosyl model complex **4** (shown in Scheme 1) was synthesized. Importantly, the iron(II)−NO

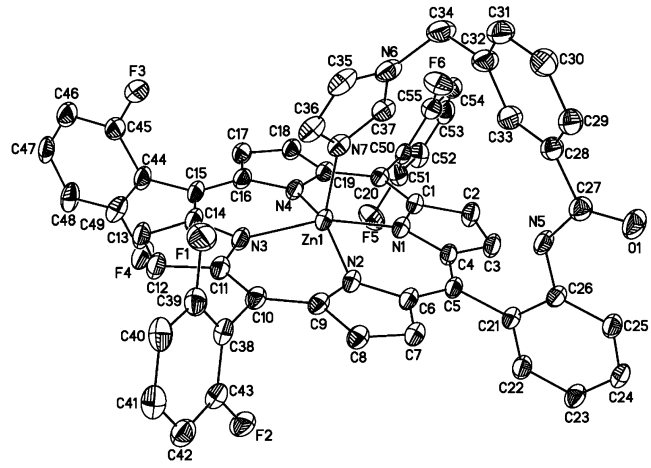

Figure 4. Molecular structure of [Zn(T*o*-F_2PP-BzIM)] showing IM bound to Zn(II) where the Zn ion is displaced form the porphyrin plane by 0.5 Å. Two CH_2Cl_2 solvent molecules are present per unit cell and have been omitted, along with all hydrogen atoms, for clarity. Selected bond lengths are reported in Table 2. A complete list of all distances and angles is provided in the Supporting Information.

Table 2. Selected Crystallographic Features of [Zn(T*o*-F_2PP-BzIM)][a]

Zn1−N1 (porphyrin)	2.077
Zn1−N2 (porphyrin)	2.095
Zn1−N3 (porphyrin)	2.064
Zn1−N4 (porphyrin)	2.073
Zn1−N7 (axial IM)	2.079
Zn1 (displacement)	0.5

[a] All values are given in Å. A complete list of distances and angles is given in the Supporting Information.

(43) Walker, F. A.; Benson, M. *J. Am. Chem. Soc.* **1980**, *102*, 5530–5538.
(44) Cormode, D. P.; Drew, M. G. B.; Jagessar, R.; Beer, P. D. *Dalton Trans.* **2008**, *47*, 6732–6741.
(45) Terazono, Y.; Patrick, B. O.; Dolphin, D. H. *Inorg. Chem.* **2002**, *41*, 6703–6710.
(46) Kojima, T.; Nakanishi, T.; Honda, T.; Harada, R.; Shiro, M.; Fukuzumi, S. *Eur. J. Inorg. Chem.,* **2009**, 727–734.

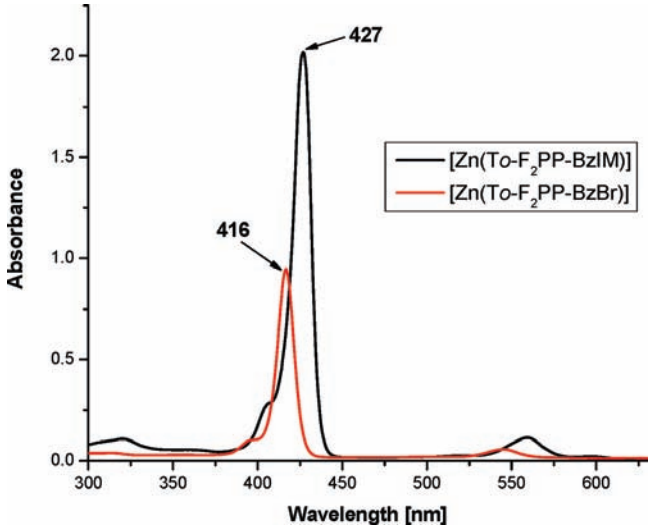

Figure 5. UV−vis spectra of the zinc complexes [Zn(T*o*-F_2PP-BzIM)] (black) and [Zn(T*o*-F_2PP-BzBr)] (red). Typical Soret and Q-band features in 5C zinc tetraphenylporphyrin complexes are seen at 427 and 559 nm, respectively, as found for the IM-bound complex. Upon replacement of IM with a noncoordinating bromine, the Soret and Q features shift to positions typically observed for 4C zinc complexes at 416 and 543 nm, respectively. This confirms the ability of the IM in ligands **L4** to coordinate to the central metal ion.

Scheme 1. Drawing of the Structure of the 6C Complex [Fe(T*o*-F_2PP-BzIM)(NO)] (**4**)

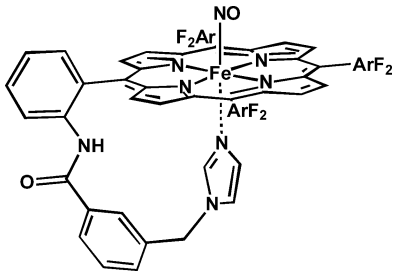

complex exhibits the Soret band at 427 nm as shown in Figure 6 (red curve), which is indicative of the formation of a stable 6C adduct in solution. The spectral features compare well with those of the 6C complex [Fe(T*o*-F_2PP)(MI)(NO)] (MI = free 1-methylimidazole), obtained in the presence of an excess of MI. In particular, the lack of a shoulder around 470 nm, which

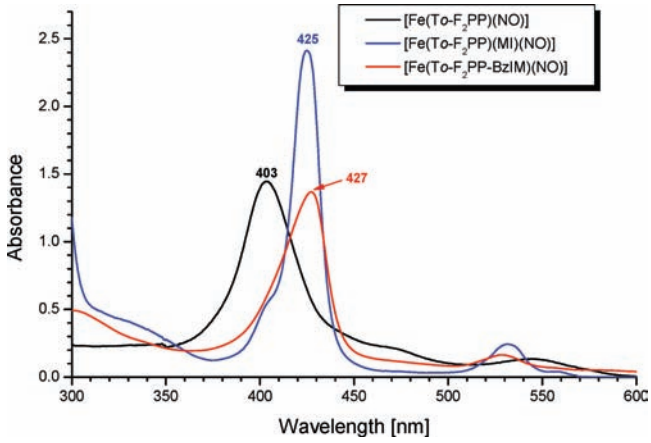

Figure 6. Electronic absorption spectra of [Fe(T*o*-F_2PP-BzIM)(NO)] (**4**, red), 5C [Fe(T*o*-F_2PP)(NO)] (black), and 6C [Fe(T*o*-F_2PP)(MI)(NO)] (MI = free 1-methylimidazole, blue).

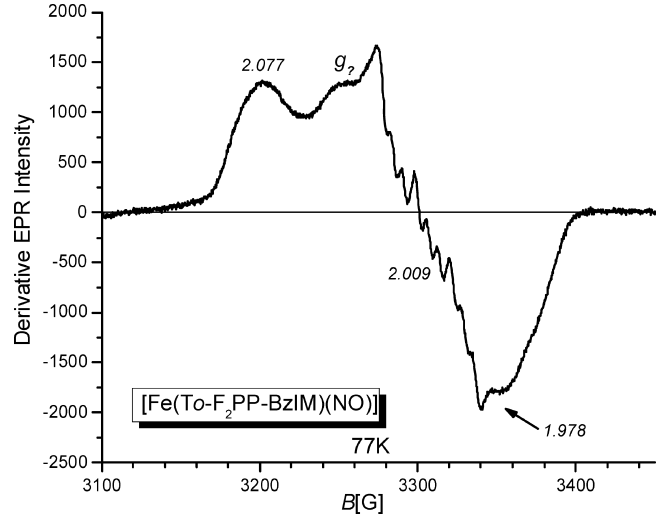

Figure 7. EPR spectrum of [Fe(T*o*-F_2PP-BzIM)(NO)] (**4**) in frozen DMSO at 77 K (^{14}N hyperfine for g(mid) [MHz]: A(NO) = 62, A(IM) = 19). A simulation of these data is shown in Figure S12 (Supporting Information). The additional signal $g_?$ is typically observed for 6C ferrous heme nitrosyls in both proteins and model complexes. See text for a detailed explanation and relevant references.

is indicative of 5C species in solution, confirms the absence of any 5C complex for the benzyl-linked compound. To further investigate the strength of the Fe−IM interaction in **4**, the EPR spectrum of this compound was recorded as shown in Figure 7. Both the observed g values of 2.08, 2.01, and 1.98, as well as the clean nine line hyperfine pattern on g(mid) with an IM-nitrogen hyperfine coupling constant of 19 MHz resemble those of well-known 6C ferrous heme nitrosyls.[32] These results confirm that **4** forms a stable 6C complex in solution where the interaction of the benzyl IM arm with the Fe(II)−NO center is strong. Neither the UV−vis data in Figure 6 nor the EPR spectrum (see fit in Figure S12, Supporting Information) indicate the presence of any 5C species in solution. To further quantify the strength of the Fe−IM interaction, solution FT-IR spectra were recorded at room temperature, since the strength of the N−O bond, represented by the N−O stretching frequency, is very sensitive to the strength of the Fe-IM interaction.[22] In 5C complexes of the type [Fe(porphyrin)(NO)], the N−O stretch ν(N−O) is observed at 1675−1700 cm^{-1} (1697 cm^{-1} for [Fe(TPP)(NO)]). Addition of a variety of free Py derivatives to [Fe(TPP)(NO)] results in weak coordination of these Py ligands and thus a moderate shift in the ν(N−O) frequency. In the case of [Fe(TPP)(4-NMe_2Py)(NO)] (4-NMe_2Py = 4-(dimethylamino)pyridine), the ν(N−O) frequency shifts down to 1653 cm^{-1} (recorded in the solid state).[37] On the other hand, upon coordination of free MI, a large shift in the ν(N−O) stretching frequency to 1630 cm^{-1} (for [Fe(TPP)(MI)(NO)]) is observed. This indicates that binding of an N-donor ligand and donation into the d_{z^2} orbital of iron weakens the Fe-NO σ-bond, and, due to the resulting reduced donation from the singly-occupied π^* orbital of NO, also weakens the N−O bond. Such an interpretation is in agreement with the experimentally observed direct correlation of the Fe−NO and N−O bond strengths and vibrational frequencies where binding of the axial N-donor ligand in fact weakens both of these bonds.[22a,b,37,47,48] In this

(47) Paulat, F; Berto, T. C.; George, S. D.; Goodrich, L. E.; Praneeth, V. K. K.; Sulok, C. D.; Lehnert, N. *Inorg. Chem.* **2008**, *47*, 11449–11451.

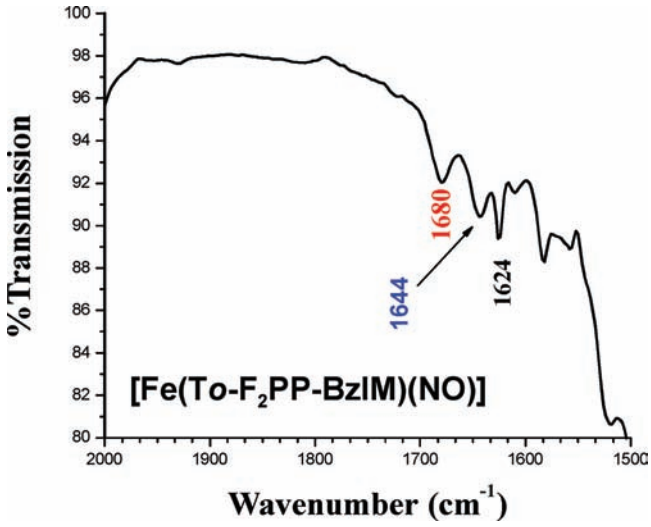

Figure 8. Solution IR spectrum of [Fe(T*o*-F_2PP-BzIM)(NO)] (**4**) showing the ν(N−O) stretching frequency at 1644 cm^{-1} (see also Figure S13, Supporting Information). This value is slightly higher than that observed for [Fe(T*o*-F_2PP)(MI)(NO)] with free MI (1624 cm^{-1}).

Table 3. Properties of 5C and 6C Ferrous Heme Nitrosyl Model Complexes[a]

complex	Soret [nm]	ν(N−O) [cm^{-1}][b]	EPR g values [c]
[Fe(TPP)(NO)][d]	405	1697	2.102/2.064/2.010(*)
[Fe(TPP)(MI)(NO)][d]	425	1630	2.079/2.004(*)/1.972
[Fe(T*o*-F_2PP)(NO)][d]	403	not det.	not det.
[Fe(T*o*-F_2PP)(MI)(NO)][d]	425	1624	not det.
[Fe(TMP-*m*Py)(NO)] [e]	406	1694	2.099/2.040/2.012(*)
[Fe(T*o*-F_2PP-C_3IM)(NO)] [e]	417	∼1686	2.087/2.002(*)/1.982
[Fe(T*o*-F_2PP-C_4IM)(NO)][e]	415	not det.	2.073/1.991(*)/1.971
[Fe(T*o*-F_2PP-BzIM)(NO)] [e]	427	1644(s)	2.077/2.009(*)/1.978
[Fe(TpivPP-IM)(NO)] [f]	415	1635(?)	2.072/2.002(*)/1.976

[a] References are included. [b] Measured at room temperature in a KBr disk. Solution data are indicated by (s). [c] Measured at lq. nitrogen temperature. The asterisk indicates the g value that shows well resolved hyperfine lines in the spectrum. [d] References 22a and b. [e] This work. [f] Reference 50. The conditions for the IR measurements are not provided.

way, binding of an axial N-donor ligand lowers the N−O stretching frequency, giving rise to the observed inverse correlation between ν(N−O) and the Fe−N(N-donor) bond strength. In the case of complexes **1**−**4** presented here, the energy of ν(N−O) can also be seen to vary significantly based on the tether employed and the specific N-donor ligand used. The IR results in Table 3 show the range of ν(N−O) energies observed based on ligand choice. Importantly, the ν(N−O) stretching frequency of **4** is observed at 1644 cm^{-1} in solution at room temperature as shown in Figure 8, which further confirms that **4** corresponds to a 6C species even in solution. Interestingly, this frequency is somewhat higher in energy compared to [Fe(T*o*-F_2PP)(MI)(NO)] (1624 cm^{-1}) and [Fe(TPP)(MI)(NO)] (1630 cm^{-1}) with bound free MI. Therefore, the IR studies show that the covalently attached benzyl-IM linker still cannot bind as strongly to the Fe(II)-NO unit as free 1-methylimidazole (MI), but that **4** forms a stable 6C complex in solution at room temperature *without the requirement for the presence of excess axial ligand*. In this regard, the N−O stretching frequency also seems to be the most sensitive probe for the strength of the Fe-IM interaction.

One problem that remains is whether **4** shows intramolecular binding of the tether as desired, or intermolecular coordination of the tether to a different complex, potentially forming dimers or large aggregates in solution. Such intermolecular coordination has been previously suggested by Momenteau for heme protein analogues in which tethers were attached to the β-pyrrole positions of the porphyrin.[10] In this case, the linkers corresponded to floppy alkyl chains. Additionally, tethers at the β-pyrrole positions should be more susceptible to intermolecular coordination due to their orientation relative to the porphyrin plane. A tether employed at the *ortho*-phenyl position of a tetraphenylporphyrin derivative is oriented toward the heme center and thus is less likely to show intermolecular coordination due to the close proximity of the tethered N-donor ligand to the Fe center of the same complex. Increasing the rigidity of the tether will further hinder this undesirable coordination. The crystal structure of the zinc complex of **L4** presented above provides further evidence that intermolecular coordination is most likely not occurring in complex **4**. To further address this issue, UV−vis dilution experiments were performed. The concentration of [Fe(T*o*-F_2PP-BzIM)(NO)] was systematically decreased until the spectra merged with the baseline, and the Soret position was determined for each concentration. As described above, the Soret band position is diagnostic for the coordination mode of the heme nitrosyl. In these experiments the Soret position remained constant (see Figure S14 in Supporting Information). This result strongly indicates that the tethered IM interacts with the iron center of the same complex. If intermolecular binding was occurring, lower concentrations should favor dissociation of the intermolecular complex and thus, a Soret shift would be observed upon concentration decrease.[10]

Our results presented above are also in agreement with recent findings of Collman and co-workers where a similarly rigid benzyl linker was used for the preparation of CcO and NorBC models, although the coordination number of the heme nitrosyls was not explicitly addressed.[19d,26,49] Nevertheless, room temperature UV−vis data shown in these reports provide evidence that the similar benzyl linker, used in conjunction with a picket fence porphyrin, also generates a 6C ferrous heme nitrosyl complex in solution. Not suprisingly, low temperature data are also in agreement with this finding. While further room temperature characterization, in particular IR spectroscopy, of these compounds is lacking, the benzyl-linked complex does appear to fulfill all the necessary requirements to generate 6C ferrous heme nitrosyls in solution as defined in this work. Besides the presence of the benzyl-IM tether, the amide-substituted TPP derivative employed in this work provides the necessary, weakly electron-poor porphyrin ligand needed to enhance IM binding to the Fe−NO unit. Only one other example of a potentially 6C iron-porphyrin NO complex with a tethered axial IM ligand is known.[50] In this case, the alkyl chain linker is attached to the β-pyrrole carbon of a picket fence porphyrin. However, whereas the EPR spectrum of this complex clearly shows binding of the IM-linker to iron(II) at low temperature, the room temperature UV−vis data exhibit the Soret band at 415 nm, which is more in agreement with the weak binding observed for **2** and **3**. A shoulder at 479 nm also indicates the

(48) Lehnert, N.; Galinato, M. G. I.; Paulat, F.; Richter-Addo, G.; Sturhahn, W.; Xu, N.; Zhao, J. Submitted for publication.

(49) Collman, J. P.; Dey, A.; Yang, Y.; Decreau, R. A.; Ohta, T.; Solomon, E. I. *J. Am. Chem. Soc.* **2008**, *130*, 16498–16499.

(50) Komatsu, T.; Matsukawa, Y.; Tsuchida, E. *Chem. Lett.* **2000**, 1060.

presence of a distinct amount of 5C species at RT in solution. Finally, dilution experiments need to be performed in this case, since β-pyrrole tailed hemes tend to form intermolecular aggregates as described above.[10]

Conclusions

As shown in this paper, the design of a truly 6C ferrous heme nitrosyl complex in solution at room temperature depends on several factors. Application of a strongly binding ligand like IM, combined with a bulky benzyl linker, is crucial for the formation of these 6C complexes. In addition, a relatively electron poor porphyrin ligand seems to facilitate IM binding, and therefore, needs to be incorporated. This can be accomplished by the addition of either fluoro substituents or amide groups to the *meso* phenyl rings of a tetraphenylporphyrin type ligand. These 6C model systems require a very specific design as compared to those employed for O_2 and CO binding studies because these diatomics do not show the strong *σ-trans* effect that is observed for NO. In this study it is demonstrated that a truly 6C ferrous heme nitrosyl can be generated in solution at room temperature in the presence of only one equivalent of the N-donor ligand, if all requirements specified above are fulfilled. The need for excess IM for the generation of 6C species, which leads to undesired side reactions including denitrosylation,[22b,24a,51] is now obsolete. Compound **4** is therefore ideally suited for reactivity studies on 6C Fe(II)−NO complexes which are currently in progress. In particular, the facile synthesis of **4** will be advantageous for application of this complex in NorBC model studies. Complex **4** is easy to prepare at relatively high total yields (2.5%) for a sophisticated porphyrin.

Interestingly, the strength of the Fe−(N-donor) bond in the benzyl-linked complex **4** is still slightly weaker than that observed for [Fe(T*o*-F_2PP)(MI)(NO)] with free MI, as evidenced by the higher ν(N−O) stretching frequency. Further studies should therefore be directed at forming even stronger Fe−(N-donor) bonds in 6C complexes as well as investigating other tethers which could potentially facilitate the formation of truly 6C ferrous heme nitrosyls in solution. This knowledge will allow for the improved synthesis of NorBC model complexes which can more effectively mimic the structure and function of the active site of this enzyme.

Acknowledgment. This work was supported by the Deutsche Forschungsgemeinschaft (DFG; grant LE 1393/1−2), the Dow Corning Corporation, and a grant from the National Science Foundation (CHE 0846235). We acknowledge Dr. Jeff W. Kampf (University of Michigan) for his X-ray crystallographic analysis of [Zn(T*o*-F_2PP-BzIM)].

Supporting Information Available: FT-IR spectra of the heme nitrosyl complexes **1**, **2**, and **4** are presented in comparison to the corresponding ferric precursor complexes, UV−vis absorption spectrum of **3**, variable concentration UV−vis spectrum of **4**, EPR spectra along with simulations for complexes **1**−**4**, complete Tables of distances and angles for [Zn(T*o*-F_2PP-BzIM)], and ^{1}H-NMR spectra of **L2**, **L3**, **L4**, and MI for comparison, complete ref 2d. This material is available free of charge via the Internet at http://pubs.acs.org.

JA904368N

(51) Lançon, D.; Kadish, K. M. *J. Am. Chem. Soc.* **1983**, *105*, 5610–5617.